

Validation of a gonio-hyperspectral imaging system based on light-emitting diodes for the spectral and colorimetric analysis of automotive coatings

FRANCISCO J. BURGOS-FERNÁNDEZ,^{1,*} MERITXELL VILASECA,¹ ESTHER PERALES,² ELÍSABET CHORRO,² FRANCISCO M. MARTÍNEZ-VERDÚ,² JOSÉ FERNÁNDEZ-DORADO,¹ AND JAUME PUJOL¹

¹Centre for Sensors, Instruments and Systems Development, Polytechnic University of Catalonia, Rambla Sant Nebridi 10, Terrassa 08222, Spain

²Department of Optics, Pharmacology and Anatomy, University of Alicante, San Vicente del Raspeig Road, San Vicente del Raspeig 03690, Spain

*Corresponding author: francisco.javier.burgos@upc.edu

Received 26 May 2017; revised 2 August 2017; accepted 7 August 2017; posted 7 August 2017 (Doc. ID 296812); published 0 MONTH 0000

In this study, a novel gonio-hyperspectral imaging system based on light-emitting diodes for the analysis of automotive coatings was validated colorimetrically and spectrally from 368 to 1309 nm. A total of 30 pearlescent, 30 metallic, and 30 solid real automotive coatings were evaluated with this system, the BYK-mac and X-Rite MA98 gonio-spectrophotometers, and also with the SPECTRO 320 spectrometer for further comparison. The results showed very precise correlations, especially in the visible range. In conclusion, this new system provides a deeper assessment of goniochromatic pigments than current approaches due to the expansion of the spectral range to the infrared. © 2017 Optical Society of America

OCIS codes: (010.1690) Color; (110.4234) Multispectral and hyperspectral imaging; (230.3670) Light-emitting diodes; (160.4760) Optical properties.

<https://doi.org/10.1364/AO.99.099999>

1. INTRODUCTION

Goniochromatic pigments, also called effect or gonioapparent pigments, are known by their appearance changes as a function of the angles of illumination and observation [1–3]. These changes can affect both color and texture, resulting in very diverse visual impressions. Accordingly, they are classified as pearlescent pigments, which mainly exhibit hue and chroma shifts, and metallic pigments, which show lightness variations; the traditional absorption pigments with a constant angular appearance are designated as solids. These pigments have acquired relevance in the industry during the last two decades, specifically in the automotive, cosmetic, printing, and packaging sectors [2,4].

The angle-dependent coatings prompted the definition of a new angular concept, the aspecular angle, which corresponds to the angle between the specular reflection and the direction of observation. Two additional concepts, the interference and aspecular lines, were subsequently generated (Fig. 1). These lines are used in the representation of the visual appearance of goniochromatic samples in a color space. The aspecular angle remains constant along the interference line, while the illumination angle is variable. However, in the aspecular line the illumination angle remains invariable. The main function of

the interference line is to reveal abrupt shifts in hue and chroma for different illumination angles (pearlescent pigments), in contrast to the aspecular line, where lightness shows the most significant variation when moving far away from the specular reflection (metallic pigments).

The growing use of coatings based on goniochromatic pigments called for the characterization at different illumination and observation geometries. Since traditional devices included just one fixed configuration, the multi-angle or gonio-spectrophotometers were created to provide more accurate assessments of effect pigments through a larger variety of measurement geometries [5]. At the same time, new standards for the complete evaluation of these pigments were issued by the German Institute for Normalization (Deutsches Institut für Normung, DIN) and the American Society for Testing Materials (ASTM) [6–8]. First, the guidelines for the analysis of metallic pigments were detailed in DIN 6175-02 and ASTM E2194. The measurement geometries described the fixed angle of illumination for the correct assessment of lightness variations along the observations angles. Since these two standards could not accurately characterize pearlescent pigments, a specific standard, ASTM E2539, was later issued. This new standard recommends two illumination angles since chroma and hue

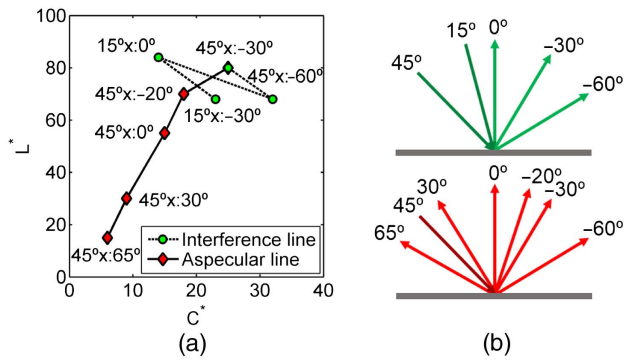


Fig. 1. Interference and aspecular lines: (a) C^* and L^* diagram showing the behavior along the different measurement geometries. (b) Measurement geometries for the interference (top) and aspecular lines (bottom).

shifts of pearlescent pigments mostly appear for different directions of illumination. Table 1 summarizes the measurement geometries recommended by these three standards.

In addition, values were established for the aperture angle (2σ) between the sample and the illumination and observation directions, defined as the angle subtended by the sensor or the light source with respect to the center of the sample. For ASTM E2194 and ASTM E2539, the angle should be $2\sigma < 8^\circ$ and equal for both directions, while DIN 6175-2 specifies the value of these angles for each measurement geometry. Furthermore, this standard differentiates between constant and variable directions, which can refer to the illumination or observation beams, depending on which has the fixed element. Therefore, the aperture angle for the constant direction must be $2\sigma \leq 5^\circ$ and for variable directions $2\sigma_{-20^\circ} \leq 4^\circ$, $2\sigma_0 \leq 4^\circ$, $2\sigma_{30^\circ} \leq 10^\circ$, and $2\sigma_{65^\circ} \leq 10^\circ$. Another condition is the CIE 1964 standard observer (10°) proposed by the Commission Internationale de l'Éclairage (CIE). The colorimetric features of goniochromatic pigments require a large field of view evaluation due to the broad spatial distribution of pearlescent and metallic particles over the sample.

In view of these developments, all large companies involved in color measurement (Datacolor, Konica Minolta, GretagMachbeth, X-Rite, BYK Additives & Instruments, Hunterlab, etc.) have launched desktop or portable gonio-spectrophotometers. The major driving force has been the interest of the automotive industry in improving the visual quality control of car finishes. Indeed, the automotive industry

Table 1. Measurement Geometries of DIN 6175-02, ASTM E2194, and ASTM E2539 Standards ([Angle of Illumination with Respect to the Normal] x : [Angle of Observation with Respect to the Normal])

Standards	Measurement Geometries
DIN 6175-02, ASTMs	$45^\circ x : -20^\circ$ $45^\circ x : 0^\circ$ $45^\circ x : 30^\circ$ $45^\circ x : 65^\circ$
ASTM E2194, E2539	$45^\circ x : -30^\circ$
ASTM E2539	$45^\circ x : -60^\circ$ $15^\circ x : 0^\circ$ $15^\circ x : -30^\circ$

is still the sector with a stronger demand for gonio-metric analysis.

Experimental gonio-spectrophotometers have also been developed with diverse operating principles and providing additional parameters: gonio-spectro-photometry based on the spectral bidirectional reflectance distribution function (sBRDF) [9,10], direct measure of the gloss at various geometries [11,12], and versatile optomechanical designs for measurements at several geometries [13]. Despite the good performance of commercial and experimental gonio-spectrophotometers, the data generally result from integrating the information of a few square millimeters of the target object. Consequently, they lack spatial resolution. For this reason, these devices can be considered to not properly estimate perceptual aspects of a surface as psychophysical experiments with real observers. At this point, the combination in hyperspectral imaging of colorimetric and textural assessments required for the special visual attributes of these coatings was considered to be the best approach to overcome these constraints.

The combination of gonio-spectrophotometers and spectral imaging systems has generated a new kind of instruments known as gonio-spectral imaging systems or multi-angle spectral imaging systems, with the main objective to obtain spectral images at different geometries. The first approaches to gonio-spectral imagery focused on the analysis of three-dimensional pieces of artwork [14–16], and later extended to two-dimensional objects such as paper and cloth samples [17,18]. The illumination system consisted of a wide spectrum light source and sets of interference filters resulting in a large and mechanically complex structure. However, it is now possible to obtain the spectral sampling directly from the light source without added elements by means of light-emitting diodes (LEDs). The advantages of LEDs are widely known: they are very efficient, present a long life cycle, evolve constantly, are comparatively economical, and have a small size. In addition, these diodes have a narrow spectral emission, and they are available at several wavelength peaks along different spectral ranges (ultraviolet, UV; visible, VIS; and infrared, IR). Another relevant advantage of LED technology is the modulation of their emission as a function of the forward current.

In the existing literature, goniochromatic pigments have only been evaluated in the VIS range of the electromagnetic spectrum, since it is the region where the main appearance shifts occur [19–21]. However, an analysis of the angular dependence at deeper layers through IR illumination would further elucidate the behavior of these pigments. Furthermore, ultraviolet lighting can contribute to a better insight into possible fluorescence. Thus, an extended spectral inspection might provide valuable information on the performance of these coatings in a broad range of bands of the electromagnetic spectrum.

This paper presents the validation of GOHYLED, a new gonio-hyperspectral imaging system based on LEDs, developed for the spectral and colorimetric evaluation of automotive coatings. This initial verification will establish the basis for future work on spatially resolved assessments. GOHYLED is specifically intended to work in an extended range from the UV to IR by using commercial, high power LEDs, in contrast

94
95
96
97
98
99
100
101
102
103
104
105
106
107
108
109
110
111
112
113
114
115
116
117
118
119
120
121
122
123
124
125
126
127
128
129
130
131
132
133
134
135
136
137
138
139
140
141
142
143
144
145
146
147
148
149
150
151

152 with conventional gonio-spectral systems that only use wide
153 spectrum light sources that exclusively cover the VIS range.

154 **2. EXPERIMENTAL SETUP**

155 The experimental setup was based on the requirements for the
156 study of automotive coatings in a wide spectral and angular
157 range specified by the DIN 6175-2, ASTM E2194-09, and
158 ASTM E2539-08 standards [6–8]. However, it might be useful
159 for other applications and configurations. Essentially, the
160 GOHYLED is composed of a spectral light source, two cameras
161 (UV-VIS and IR) that cover the 368–1309 nm range, and two
162 rotation stages with a total rotation angle of 180° in both
163 observation and illumination directions (Fig. 2). All elements
164 were controlled through a purpose-built graphical user interface
165 developed with MATLAB R2013a, which allows the individual
166 and synchronized use of the light source, cameras, and motor-
167 ized rotation stages.

168 **A. Light Source**

169 The light source consists of 28 high power surface-mounted-
170 device (SMD) LED clusters of different peak wavelengths that
171 spectrally illuminate the sample and a linear actuator that
172 sequentially positions each cluster in front of it. A white

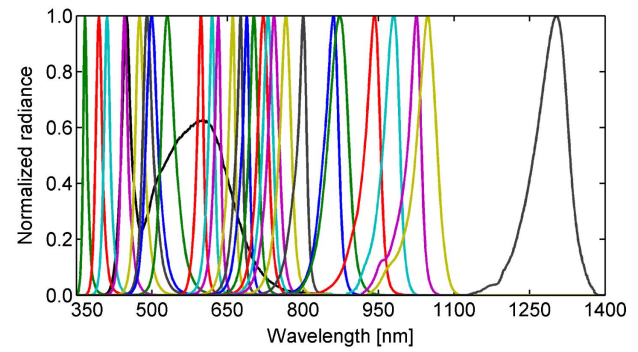


Fig. 3. Normalized spectral radiance of the LEDs included in the GOHYLED system.

LED cluster was also incorporated for the subsequent spatial
evaluation of texture, which is not included in this work.
The clusters are composed of three or six LEDs, depending
on the radiance emitted. A lens to increase the amount of light
over the sample was also incorporated. Figure 3 shows the
normalized spectral radiance, and Table 2 contains the part
number and peak wavelengths of the whole set of LEDs.

The LEDs were purchased from Roithner LaserTechnik
GmbH (Part numbers RLCU and SMB1N) and Lumileds
Holding B.V. (Part numbers LX). The UV-VIS LEDs
(368–774 nm) presented a mean spectral step between con-
secutive peak wavelengths of around 20 nm, whereas in the
IR (807–1309 nm), this value increased to 40 nm. The
FWHM in the UV-VIS range varies from 10 to 37 nm and
from 30 to 80 nm in the IR. The higher FWHM and the sub-
sequent overlapping of the spectra in the IR range partially
compensated the larger distance among peak wavelengths.
Even though it causes a coarser sampling, the broader
FWHM is a typical feature of current IR solid-state technology
that is still unsolved. Moreover, IR LEDs present less variety of
wavelengths, especially those of high power—thus the signifi-
cant gap before the spectrum with a peak wavelength of
1309 nm in Fig. 3.

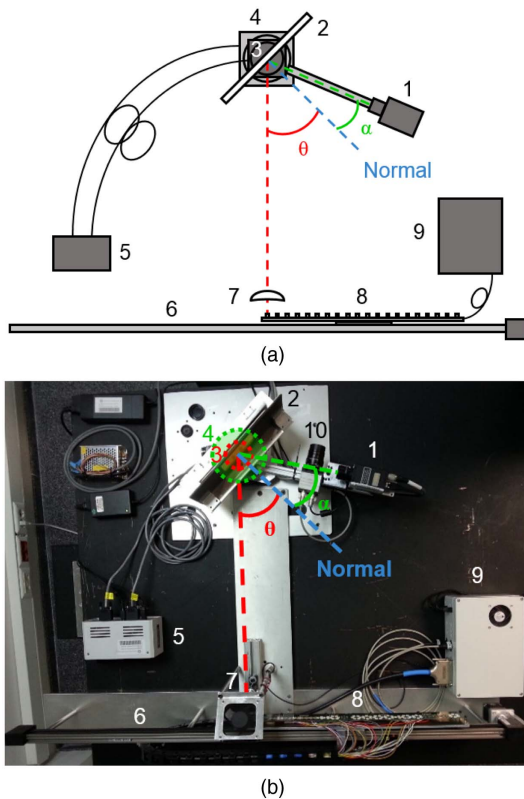


Fig. 2. Developed gonio-hyperspectral imaging system based on LEDs represented in (a) a layout and in (b) a picture: 1, UV-VIS camera; 2, sample holder; 3, 8MR191-30 rotation stage; 4, 8MR191-30-28 rotation stage; 5, rotation stages controller; 6, linear actuator; 7, lens; 8, LED clusters; 9, light source controller and power supply; 10, IR camera, which is not represented in (a). θ refers to the illumination angle controlled by the 8MR151-30 rotation stage and α to the observation angle handled by the 8MR191-30-28 rotation stage.

Table 2. Part Numbers and Peak Wavelengths (λ_p) of the 28 Types of LEDs

Part Number	λ_p [nm]	Part Number	λ_p [nm]
RLCU-440-365	368	SMB1N-700	709
RLCU-440-390	397	RLCU-440-720	724
RLCU-440-410	411	SMB1N-735	735
LXML-PR01-0500	446	SMB1N-750	748
LXML-PB01-0040	476	SMB1N-770	774
SMB1N-490	489	SMB1N-810D	807
LXML-PE01-0070	498	SMB1N-850D	867
LXML-PM01-0100	528	SMB1N-870	885
LXML-PL01-0060	601	SMB1N-940D	952
LXM2-PH01-0070	622	RLCU-440-970	984
LXM2-PD01-0050	634	RLCU-440-1020	1033
LXM3-PD01	663	RLCU-440-1050	1052
SMB1N-670D	678	SMB1N-1300	1309
SMB1N-690D	693	LXW8-PW40	449/599*

*Peak wavelengths of the two peaks for the white LEDs.

The use of high power LEDs was driven by the aperture angles recommended by the standards. To achieve such small angles, the illuminating and sensing areas should have been extremely reduced, limiting the evaluation to a minute fraction of the samples. However, one of the objectives of this work was to evaluate bigger areas than current devices and to obtain spatially resolved images. To this end, the LEDs were placed at a distance of 580 mm in order to leave enough free space for the rotation of the acquisition arm around the sample. But the long distance and the angle of emission of the LEDs (120°) resulted in a low illumination of the sample. To solve this issue, a plano-convex lens from Edmund Optics (stock #67-228) with a focal length of 75 mm, a diameter of 50 mm, and a transmittance of 90% from 200 to 1300 nm was selected. The relative position between the LEDs and the lens was out of focus to avoid an image of the LED chips to form on the sample. The lens back surface was finally placed 25 mm from the LEDs; this was experimentally determined and ensured a uniform illumination over the sample. This configuration of the light source produced an aperture angle of 4.69°, which was below the maximum tolerance of the ASTM E2194 and E2539 (8°) and DIN 6175-2 (5°) standards, considering for the latter the illumination beam as the constant direction.

The linear actuator ZLW-0630-02-B-60-L-1000 from Igus S.L., and a stepper motor SY42STH47-1206A from Changzhou Songyang Machinery & Electronics Co., Ltd., executed the sequential positioning of the LED clusters, resulting in a minimum step of 140 μm. Each LED cluster was switched on only when it was placed in front of the sample and behind the lens. The images were then acquired by the camera, the LEDs were switched off, and the next cluster was placed in the same position to repeat the process. With this method, only one LED cluster was switched on at a time.

B. Imaging Sensors

Table 3 contains the technical features of the two cameras used. The acquisition unit included a CM-140 GE-UV monochromatic CCD camera from JAI AS, with enhanced UV sensitivity, and a GMUV42528C 2.8/25 mm quartz lens from GOYO OPTICAL Inc. selected specifically for its high transmittance from 200 to 1300 nm. The InGaAs camera was a Hamamatsu C10633-23 with a lower spatial resolution and exposure time and no available gain factor. A Kowa LM12HC-SW 1.4/12.5 mm SWIR lens with high transmission from 800 to 2000 nm was coupled to this camera. The spatial resolution of the IR camera did not pose a problem since the validation of the proposed system was performed by means of averaged reflectances of the images. However, it can limit future spatial evaluations.

The acquisition was made in a two-step process. The UV-VIS camera was employed to acquire images when using

Table 3. Technical Features of the Cameras

Camera	UV-VIS	IR
Spectral range [nm]	200–1000	900–1650
Sensor size [px]	1392 × 1040	320 × 256
Bit depth	10	14

the LED clusters with peak wavelengths from 368 to 952 nm, and the IR camera for peak wavelengths from 984 to 1309 nm. The images for the whole set of measurement geometries were first captured with the UV-VIS and second with the IR camera.

The aperture angles of the observation stage also conformed to the standards. The minimum distance between the sample and the cameras was based on the maximum diameter of the entrance pupil. Since it can be obtained dividing the focal length by the minimum F-number, the lenses of both cameras presented the same value of 8.93 mm. However, the distance to the sample was different for each camera because the position of the entrance pupil was different for each lens, at 14.1 mm for the UV-VIS lens and at 10.7 mm for the IR lens, both inward. Consequently, the minimum distances between the sample and the outer part of the cameras' lenses were 113.8 mm for the UV-VIS and 117.1 mm for the IR. Finally, the UV-VIS camera was positioned at 218 mm from the sample to increase the area observed; this resulted in one aperture angle of 2.20°. The IR camera was located at 129 mm from the sample to avoid any collision with the sample holder; this distance variation generates an aperture angle of 3.66°. A longer distance was not used for this camera because of its wider field of view and lower spatial resolution. Both cameras conformed to the tolerance of the ASTM E2194 and E2539 (8°) and DIN 6175-2 (4°) standards, considering for the latter the observation beam as the variable direction. Although these standards only regulate the measurement of goniochromatic pigments in the VIS range, the same conditions were applied to the IR due to the lack of regulations in this range.

To capture images within the dynamic range of the cameras, exposure time and gain varied throughout the measurement geometries and for the different acquisition channels. Besides the emission power of each LED cluster, the spectral sensitivity of the cameras and the angular distance between the illumination and observation direction also conditioned these parameters.

C. Motorized Rotation Stages

The changeable angular positioning was obtained using two motorized rotation stages manufactured by STANDA Ltd, the 8MR151-30 and the 8MR191-30-28. Both have a rotation range of 360°, an angular resolution of 0.01°, and a central aperture of 30 mm. At the top, the 8MR151-30 stage controls the illumination angle by rotating the sample, while at the bottom, the 8MR191-30-28 controls the observation direction by positioning the cameras around the sample. Figure 2 shows a graphical description of the angular positioning of each stage.

3. METHODS

A. Samples

A total of 30 pearlescent, 30 metallic, and 30 solid samples were selected; they presented a rectangular size between 90 mm × 150 mm and 100 mm × 200 mm. The 90 samples originated from AUDI AG, BASF SE, and PPG Industries Inc. commercial car paints. In addition to the measurements carried out with the GOHYLED system, these samples were measured with the BYK-mac (BYK-Gardner GmbH) and X-Rite MA98 (X-Rite Inc.) gonio-spectrophotometers and also the

T3:1
T3:2
T3:3
T3:4

246
247
248
249
250
251
252
253
254
255
256
257
258
259
260
261
262
263
264
265
266
267
268
269
270
271
272
273
274
275
276
277
278
279
280
281
282
283
284
285
286
287
288
289
290
291
292
293
294
295
296
297
298
299
300
301

302 SPECTRO 320 spectrometer (Instruments Systems GmbH)
303 for further comparisons.

304 **B. Multi-Angle Color Measurement**

305 The GOHYLED system was designed and built considering
306 the measurement geometries, aperture angles, and CIE stan-
307 dard observer recommended by the DIN 6175-2, ASTM
308 E2194-09, and ASTM E2539-08 standards (Table 4). The
309 aperture angle for the UV-VIS camera was eventually smaller
310 because the diaphragm size of the camera lens was diminished
311 ($f/11$) to enhance the focus at the 368–952 nm spectral range.
312 In contrast, the IR camera used a greater diaphragm ($f/2.8$) to
313 ensure a good signal-to-noise ratio, since IR LEDs had lower
314 power than VIS LEDs. Furthermore, the focus was less critical
315 than in the UV-VIS region because the IR camera operated
316 with LEDs in a range of only 300 nm. The measurement area
317 or region of interest (ROI) was determined for the UV-VIS
318 camera because its field of view was more limited.

319 The major benefit of conforming to ASTM and DIN spec-
320 ifications is the possibility of performing a precise comparison
321 of readings among instruments of different optical design. The
322 measurements obtained with the GOHYLED system were
323 compared to those of the BYK-mac and X-Rite MA98 gonio-
324 spectrophotometers. These devices are calibrated for all the
325 geometries against ceramic standards of the British Ceramic
326 Research Association, known as BCRA tiles. The BYK-mac
327 conforms only to the DIN 6175-2 and ASTM E2194 stan-
328 dards, whereas the X-Rite MA98 and the GOHYLED conform
329 to the three standards (DIN 6175-2, ASTM E2194, and
330 ASTM E2539). With a fixed illumination direction, the
331 BYK-mac is particularly suitable for the evaluation of metallic
332 pigments, but it cannot characterize the changes of hue and
333 chroma that appear in pearlescent pigments for different illu-
334 mination directions. Similarly to the GOHYLED, the BYK-
335 mac performs the spectral sampling by means of LEDs and
336 can evaluate sparkle and graininess, both textural effects of
337 goniochromatic pigments. On the other hand, the X-Rite
338 MA98 can produce complete assessments of pearlescent and
339 metallic pigments since it includes the 45° and 15° illumination
340 angles required by the standards. It also includes other obser-
341 vation angles outside the conventional plane of illumination/
342 observation, and a diffraction grating performs the spectral
343 sampling. Besides the standard, the BYK-mac and X-Rite
344 MA98 also perform evaluations at the $45^\circ \times -60^\circ$ measure-
345 ment geometry. Therefore, the spectral and colorimetric results
346 obtained with the GOHYLED system were fully comparable to
347 those of the X-Rite MA98, whereas only the geometries sug-
348 gested by the DIN 6175-2 and ASTM E2194 standards,
349 $45^\circ \times -30^\circ$, $45^\circ \times -20^\circ$, $45^\circ \times 0^\circ$, $45^\circ \times 30^\circ$, and $45^\circ \times 65^\circ$,

plus $45^\circ \times -60^\circ$, were used to compare with the results of the
BYK-mac.

352 **C. Measurement Stability and Repeatability**

353 The stability and repeatability of the measurement procedure
354 were also evaluated through the acquisition of images of a white
355 reference BN-R98-SQ10C from Gigahertz Optik GmbH at
356 the geometry of $45^\circ \times 0^\circ$ with both cameras and the quantifi-
357 cation of the mean digital level variation.

358 First, the stability of all the spectral channels was examined
359 by switching every LED cluster on and off 10 times and each
360 time capturing 10 images, which were subsequently averaged.
361 The purpose of these tests was to accurately reproduce the final
362 measurement mechanism, in which the LED clusters were used
363 as flashes of light. Next, the influence of the sample positioning
364 on the holder was evaluated. This study encompassed the com-
365 parison of measurements with and without the replacement of
366 the sample among repetitions.

367 In order to reduce other sources of bias such as temporal
368 noise, sets of three, five, and 10 averaged frames were tested
369 for the two cameras at the geometries of $45^\circ \times -60^\circ$,
370 $45^\circ \times -30^\circ$, $45^\circ \times -20^\circ$, $45^\circ \times 0^\circ$, $45^\circ \times 30^\circ$, and $45^\circ \times 65^\circ$,
371 using the white reference mentioned before.

372 The proposed system also dealt with spatial noise removal,
373 in this case by applying Eq. (1) to each acquired image:

$$I_C(i, j) = k \frac{I(i, j) - I_B(i, j)}{I_U(i, j) - I_B(i, j)}, \quad (1)$$

374 where $I_C(i, j)$, $I(i, j)$, $I_B(i, j)$, and $I_U(i, j)$ correspond to the
375 digital levels of the corrected, raw, background or dark, and
376 uniform field or white reference images, respectively; k is
377 the calibrated reflectance of the reference provided by the
378 manufacturer. $I(i, j)$, $I_B(i, j)$, and $I_U(i, j)$ images were always
379 acquired in the same conditions of exposure time and gain,
380 which change for each acquisition channel and measurement
381 geometry. Images of the calibrated white reference were cap-
382 tured and used as uniform field targets, as well as dark or back-
383 ground images with all LEDs turned off. The results derived
384 from Eq. (1) were directly expressed as reflectance images.

385 The evaluation of the positioning repeatability of the rota-
386 tion stages was carried out by means of the UV-VIS camera
387 attached to the 8MR191-30-28 stage through the acquisition
388 arm at the distance previously calculated (218 mm from the
389 sample). A graph paper divided into 1 mm squares was used
390 as the sample to quantify the deviation of the image recorded.
391 Positioning tests were performed for rotations of 30° , 10° , and
392 5° , first with one of the two elements fixed and afterwards mov-
393 ing both; each rotation displacement was assessed three times.

394 **D. Extraction of Reflectance Spectra and**
395 **Colorimetric Data**

396 The spectral and color appearance data were retrieved by means
397 of a purpose-developed image processing program using
398 MATLAB R2013a. Its main functions were to calculate the
399 reflectance spectra, spectral fitting metrics, chromatic coordi-
400 nates, and color differences.

401 Reflectance images were obtained by means of Eq. (1).
402 Throughout the whole spectral range of the GOHYLED sys-
403 tem (368–1309 nm), the average reflectance values were also

Table 4. F-Number, Aperture Angles (2σ), Spatial Resolutions (SR), and Regions of Interest (ROI) for Each Camera

Camera	F-Number	2σ [°]	SR [px/mm]	ROI [mm]
UV-VIS	$f/11$	0.56	28	50×37
IR	$f/2.8$	1.83	3	50×37

determined for three ROIs: the ROI detailed in Table 4 and the ROIs of the BYK-mac and the X-Rite MA98 gonio-spectrophotometers with diameters of 23 and 12 mm, respectively. Although the ROIs of the GOHYLED system are square or rectangular and those of the two gonio-spectrophotometers are circular, the differences were considered negligible. These spectra were finally interpolated from 400 to 700 nm with a step of 10 nm by applying a cubic spline algorithm [22,23], on account of the input spectral range needed for calculating the colorimetric values and color differences with respect to those of the BYK-mac and X-Rite MA98. Regarding the IR range, the spectra were validated with the measurements carried out with the SPECTRO 320 spectrometer and the telescopic optical probe TOP 100 from Instrument Systems GmbH and a halogen lamp at the geometries of $45^\circ \times :30^\circ$, $45^\circ \times :0^\circ$, and $15^\circ \times :0^\circ$. This device and all its accessories are calibrated against standards of the National Institute of Standards and Technology (NIST) and the Physikalisch-Technische Bundesanstalt (PTB). The spectral range went from 700 to 1309 nm with a step of 10 nm. No additional geometries were assessed since these were considered sufficiently representative and also due to the lack of automation of the measurement process.

Additionally, the comparison of the spectra between the GOHYLED system and the BYK-mac, the X-Rite MA98, and the SPECTRO 320 was completed through the mean absolute error (MAE), root mean square error (RMSE) [24,25], and goodness-of-fit coefficient (GFC) [26,27]. These metrics were chosen because they are commonly used when comparing reconstructed spectral data [25,27,28]. Moreover, the combination of the MAE and RMSE is useful to detect whether values are caused by generalized large errors (RMSE \sim MAE) or by a few errors greater than MAEs, such as outliers (RMSE $>$ MAE); both parameters are in the same units as the analyzed data. On the other hand, the GFC is a relative measure between 0 and 1 based on Schwartz's inequality, commonly used when comparing spectra and, especially, color differences [Eq. (2)]. According to the scale commonly linked to this parameter [27], a GFC ≥ 0.9950 is considered "colorimetrically accurate," a GFC ≥ 0.9990 a "good spectral fitting," and a GFC ≥ 0.9999 an "excellent spectral fitting":

$$\text{GFC} = \frac{|\sum_i^n r_o(\lambda_i) r_e(\lambda_i)|}{\sqrt{\sum_i^n [r_o(\lambda_i)]^2 \sum_i^n [r_e(\lambda_i)]^2}}, \quad (2)$$

where $r_o(\lambda_i)$ is the original spectrum and $r_e(\lambda_i)$ is the estimated spectrum, both evaluated at the same wavelength λ_i ; n is the total amount of wavelengths considered.

The colorimetric evaluations were performed under the CIELAB color space [29,30]. The CIE standard illuminant selected was D65, similarly to BYK-mac and X-Rite MA98. Color differences between these devices and the GOHYLED were calculated with the CIEDE2000 [31,32] and AUDI2000 [33] color-difference formulas. The CIEDE2000 color-difference formula is defined as

$$\Delta E_{00} = \left[\left(\frac{\Delta L'}{k_L S_L} \right)^2 + \left(\frac{\Delta C'}{k_C S_C} \right)^2 + \left(\frac{\Delta H'}{k_H S_H} \right)^2 + R_T \left(\frac{\Delta C'}{k_C S_C} \right) \left(\frac{\Delta H'}{k_H S_H} \right) \right]^{\frac{1}{2}}, \quad (3)$$

where $\Delta L'$, $\Delta C'$, and $\Delta H'$ are differences of lightness, chroma, and hue between two colors, respectively. This formula included parametric factors k_L , k_C , and k_H for weighting lightness, chroma, and hue differences, respectively, according to the application. These three parameters are equal to 1 under the reference conditions proposed by the CIE [34,35]. In addition, three weighting functions, S_L , S_C , and S_H for each lightness, chroma, and hue, were also included. Finally, the rotation term R_T was added to improve the performance for blue colors. The improved performance for objects that exhibit lightness values higher than 100 was a decisive factor, since this phenomenon is very common in goniochromatic pigments, especially under direct illumination conditions.

On the other hand, the AUDI color-difference formula was specially developed for the approval of goniochromatic paint batches as follows:

$$dE'_\gamma = \left[\left(\frac{dL'_\gamma}{k_{dL} s_{dL_\gamma}} \right)^2 + \left(\frac{dC'_\gamma}{k_{dC} s_{dC_\gamma}} \right)^2 + \left(\frac{dH'_\gamma}{k_{dH} s_{dH_\gamma}} \right)^2 \right]^{\frac{1}{2}}. \quad (4)$$

The main difference with respect to the CIEDE2000 is that, in this case, the weighting functions (s_{dL_γ} , s_{dC_γ} , s_{dH_γ}) depend on the measurement geometry.

4. RESULTS AND DISCUSSION

The spectral reconstruction of the 90 samples comprised the entire spectral range of the GOHYLED system, from 368 to 1309 nm, with 28 acquisition channels, eight color measurement geometries, and three ROIs. Figure 4 shows two reflectance images of a pearlescent pigment at the geometries of $45^\circ \times : -30^\circ$ and $45^\circ \times : -20^\circ$ and for the LED cluster with a peak wavelength of 476 nm. The illumination gradient was not removed when dividing by the image of the white reference because it has a matte finish, whereas the automotive coatings were glossy. At this stage, a glossy white reference was not used to reach a more precise comparison with the BYK-mac and the X-Rite MA98, which also employ a matte white reference.

Figure 5 exhibits the reflectance spectra, and Fig. 6 the C^* versus L^* of three samples where the pearlescent, metallic, and solid effects were more noticeable. Measured samples showed the expected theoretical behavior that was also confirmed by the commercial devices. Chroma shifts were more evident in pearlescent samples due to variations of the reflectance spectrum in relation to wavelength and to the interference and aspecular lines. Luminance changes in goniochromatic samples

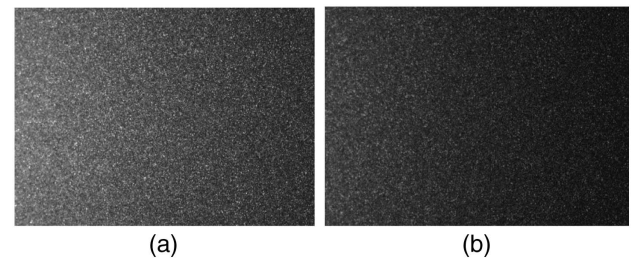
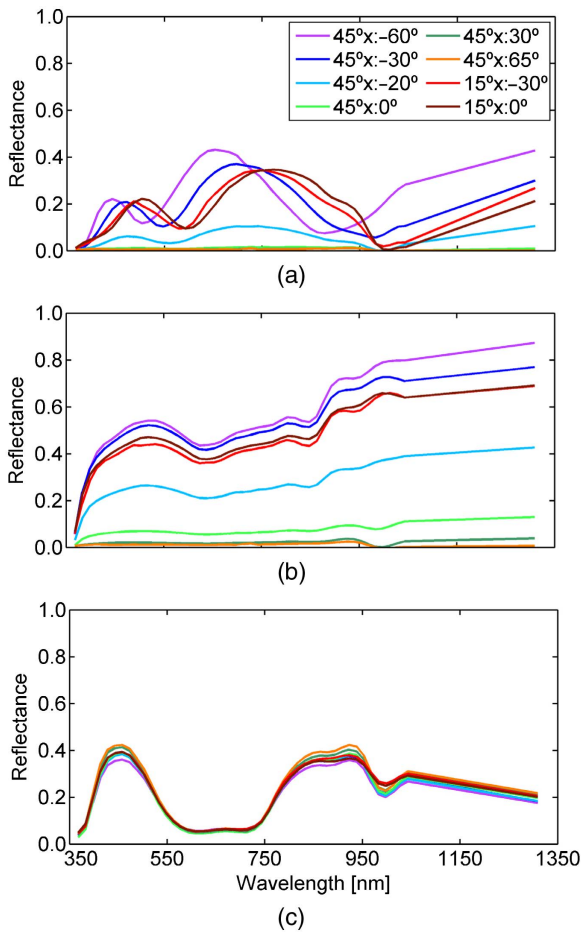


Fig. 4. Reflectance images of a pearlescent pigment at the geometries of (a) $45^\circ \times : -30^\circ$ and (b) $45^\circ \times : -20^\circ$ for the LED cluster with a peak wavelength of 476 nm.

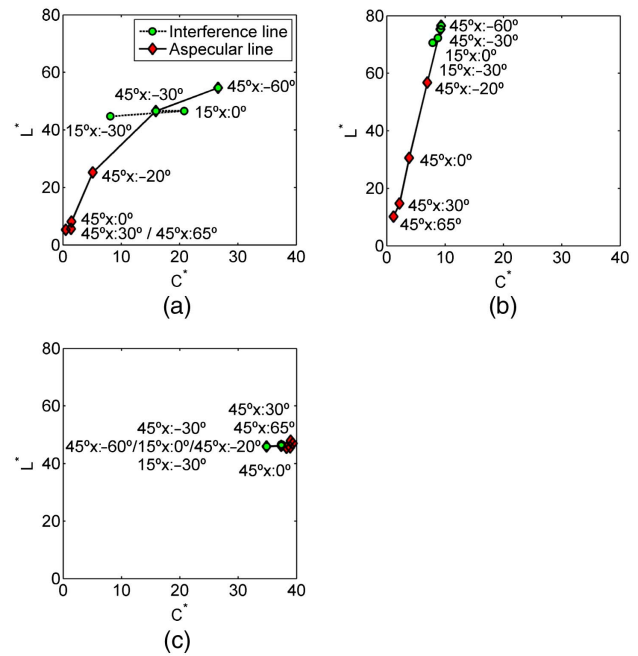


F5:1 **Fig. 5.** Reflectance spectra of (a) pearlescent, (b) metallic, and
 F5:2 (c) solid samples at $45^\circ \times -60^\circ$, $45^\circ \times -30^\circ$, $45^\circ \times -20^\circ$, $45^\circ \times 0^\circ$,
 F5:3 $45^\circ \times 30^\circ$, $45^\circ \times 65^\circ$, $15^\circ \times -30^\circ$, and $15^\circ \times 0^\circ$.

494 were recorded as variations in reflectance [Figs. 5(a) and 5(b)]
 495 and lightness [Figs. 6(a) and 6(b)]. Although this phenomenon
 496 is the main attribute of metallic samples, it was also observed in
 497 pearlescent samples because pearlescent pigments employed in
 498 automotive coatings are commonly mixed with metallic particles
 499 to integrate the two effects in one single paint. With
 500 regard to solid samples, the spectral reflectance, chroma, and
 501 luminance remained stable in the eight geometries with only
 502 minor fluctuations [Figs. 5(c) and 6(c)]

503 Figures 5(a), 5(b), 6(a), and 6(b) show that reflectance and
 504 lightness values, respectively, were higher at the geometries
 505 adjacent to the specular reflection ($45^\circ \times -60^\circ$, $45^\circ \times -30^\circ$,
 506 $15^\circ \times -30^\circ$, and $15^\circ \times 0^\circ$) and decreased drastically in the case
 507 of the furthest geometries. On the other hand, the most signifi-
 508 cant changes in the spectral profile emerged when comparing
 509 the measurements of geometries with the illuminant at differ-
 510 ent positions: $45^\circ \times -60^\circ$ and $45^\circ \times -30^\circ$ versus $15^\circ \times -30^\circ$
 511 and $15^\circ \times 0^\circ$. These geometries are recommended for the
 512 evaluation of color change due to pearlescent pigments [8].

513 The following results are based on the average reflectance of
 514 the images for a more precise comparison with the BYK-mac
 515 and X-Rite MA98, since they do not offer pixel-wise reflectance
 516 data. At this stage, the spatially resolved images were not



F6:1 **Fig. 6.** C^* and L^* diagrams of (a) pearlescent, (b) metallic, and
 F6:2 (c) solid samples at $45^\circ \times -60^\circ$, $45^\circ \times -30^\circ$, $45^\circ \times -20^\circ$, $45^\circ \times 0^\circ$,
 F6:3 $45^\circ \times 30^\circ$, $45^\circ \times 65^\circ$, $15^\circ \times -30^\circ$, and $15^\circ \times 0^\circ$.

517 exploited because the main objective of this work was to
 518 perform a preliminary spectral and colorimetric validation of
 519 performance by means of comparing the new system against
 520 two commercial gonio-spectrophotometers. The next stage will
 521 focus on spatial features of goniochromatic pigments such as
 522 sparkle, graininess, and mottling under broad-band and nar-
 523 row-band light sources. The deeper penetration of IR light will
 524 provide a more accurate analysis of the goniochromatic particles
 525 located at deeper layers of the coating and will also contribute
 526 to quantify their influence on the total appearance of the pig-
 527 ment. Preliminary results have revealed a better discrimination
 528 of some spatial attributes in the IR range due to the removal of
 529 sparkle at this spectral region and for coatings of different
 530 thickness.

531 **A. Stability and Repeatability Performance**

532 The results for stability assessments demonstrated excellent
 533 performance of all spectral channels with differences among
 534 repetitions below 5.75% for the UV-VIS camera and under
 535 1.97% for the IR camera. The most outstanding shifts due
 536 to the influence of the sample positioning appeared when
 537 replacing it, but they were considered minor fluctuations
 538 because the deviation values never exceeded 4%.

539 Temporal noise analysis led to maximum differences
 540 below 1% when comparing the mean digital levels of the three
 541 sets of frames. This percentage was calculated with respect
 542 to the maximum digital level of each camera: 1023 for the
 543 UV-VIS and 16383 for the IR. The minimum number of
 544 frames (three) was selected for each acquisition.

545 The positioning repeatability evaluation of the rotation
 546 stages revealed a maximum positioning deviation under 1%,
 547 which confirmed the accuracy of both stages.

B. Spectral Performance in the Visible Range

The first data evaluated were the spectral reconstructions from 400 to 700 nm by means of the MAE, RMSE, and GFC. We should stress that the MAEs and the RMSEs are expressed as reflectance differences. These three metrics were computed for the three ROIs and the three pigment categories. The performance among ROIs was very similar and validated the use of the maximum measurement area without undermining the fitting; therefore, only the results for the full ROI are shown. Figure 7 plots the mean values considering the different geometries for the three types of samples; each bar includes the standard error as a measure of uncertainty.

The precise reconstructions obtained with the developed system revealed that all the mean values of MAE and RMSE were below 0.03 and very similar, which means that very few outliers were found. The mean GFCs, all above 0.9900, also proved the color accuracy. The GOHYLED system and the BYK-mac exhibited slightly more similar behavior than the X-Rite; in terms of MAE and RMSE this result was similar to the result of comparing the two commercial devices. With regard to the scale for the GFC, the evaluation of pearlescent and solid pigments can be considered “colorimetrically accurate” since the mean values of this parameter were above

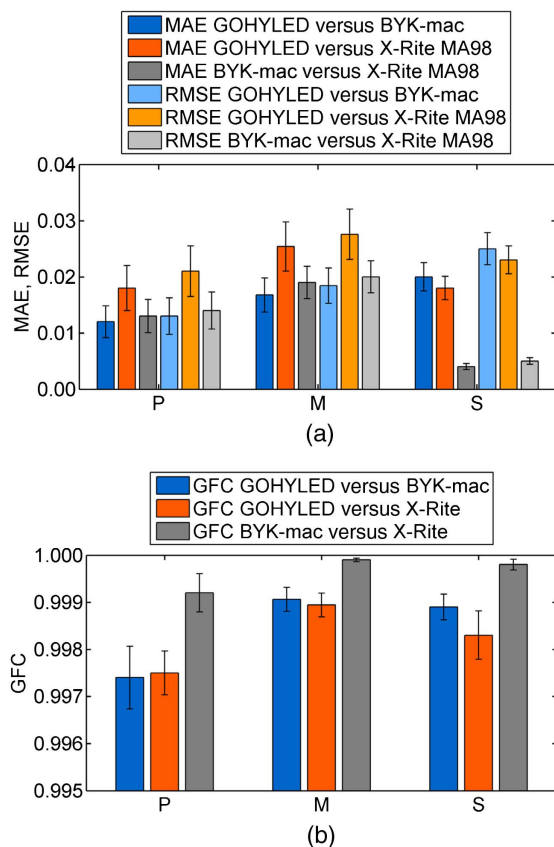


Fig. 7. Mean values of (a) MAEs and RMSEs and (b) GFCs for the spectral reconstruction of the GOHYLED system with respect to the BYK-mac and the X-Rite MA98 and the comparison between two gonio-spectrophotometers. The three metrics were plotted for pearlescent (P), metallic (M), and solid (S) samples. The error bars represent the standard error.

0.9950, while metallic pigments attained “good spectral fitting” with values slightly above 0.9990. These last subsets of pigments also achieved correlations very similar to the correlations between the two gonio-spectrophotometers. In agreement with previous studies [36,37], the measurement geometries closer to the specular reflection ($45^\circ \times -60^\circ$, $45^\circ \times -30^\circ$, $15^\circ \times 30^\circ$, and $15^\circ \times 0^\circ$) resulted in larger differences. At these geometries, the amount of light reflected is very high and any small variation in position or configuration can produce substantial deviations of the results.

Color differences again showed better correlations between the GOHYLED system and the BYK-mac, although the deviations with respect to the X-Rite MA98 were less noticeable than in the fitting metrics (Fig. 8). The greatest spectral and colorimetric match obtained for the GOHYLED system and the BYK-mac was probably due to the use of the same spectral filtering technique, i.e., LEDs, with similar spectral features such as the peak wavelength and the FWHM.

In general, the mean CIEDE2000 values were below 2 units with all instruments and for the three kinds of samples. These colorimetric differences remained within the ranges proposed in a previous study [38], where the authors suggested to widen color tolerances when using newer versions of standardized color-difference formulas such as the CIEDE2000; this study did not cover non-standard color-difference equations such as the AUDI2000. This tolerance proposal was based on the large numbers of factors that determine the reproduction of automotive coatings: add-on parts, closeness to the specular angle, $L^* > 100$, and visual texture. Considering all these circumstances, they recommended to apply a multiplication factor between 1.5 and 3 with respect to the visual discrimination threshold, traditionally equal to 1.

In contrast, the AUDI2000 color differences were larger, particularly for solid samples. It is known that this color-difference formula is stricter than the CIEDE2000, particularly for solid pigments, because their appearance is considered less complex and easier to reproduce than for goniochromatic pigments. Since the solid samples employed in this study

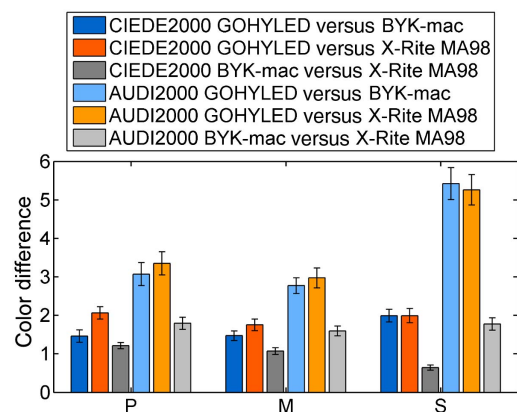


Fig. 8. Mean CIEDE2000 and AUDI2000 color differences of the GOHYLED system with respect to the BYK-mac and the X-Rite MA98 and also the comparison between the two gonio-spectrophotometers for the full ROI. Both metrics were plotted for pearlescent (P), metallic (M), and solid (S) samples. The error bars represent the standard error.

571
572
573
574
575
576
577
578
579
580
581
582
583
584
585
586
587
588
589
590
591
592
593
594
595
596
597
598
599
600
601
602
603
604
605
606
607
608

609 showed surfaces with more gloss than the pearlescent and
 610 metallic, any minor variation in the configuration could cause
 611 considerable variations among instruments. With regard to
 612 Fig. 8, the values shown were calculated considering the whole
 613 set of measurement geometries.

614 The comparisons with the GOHYLED system were very
 615 similar to the comparison between the two commercial
 616 gonio-spectrophotometers, especially for pearlescent and met-
 617 allelic pigments in terms of MAE, RMSE, and CIEDE2000.
 618 We can thus infer that the BYK-mac and X-Rite MA98 present
 619 differences of a magnitude similar to the GOHYLED.
 620 However, the correlation of their measurements for solid pig-
 621 ments was better than with the proposed instrument. Indeed,
 622 solid pigments showed a very glossy surface, to which the
 623 GOHYLED system seemed to be more sensitive than the
 624 gonio-spectrophotometers. Since the ROIs employed were
 625 the same as those of the commercial devices, the illumina-
 626 tion path might be considered responsible for these differences.
 627 A collimated beam and/or a smaller aperture could increase the
 628 fitting with the reference devices. Finally, even though the cor-
 629 relations presented provide valuable information, further vali-
 630 dation by means of psychophysical experiments is still needed.

631 C. Spectral Performance in the Infrared Range

632 Figure 9 shows the results of the validation of the IR range from
 633 700 to 1309 nm. In this case, only the spectral fitting metrics
 634 (MAE, RMSE, and GFC) were computed. Besides the full
 635 ROI, the ROI of 12 mm was also analyzed, since it was the
 636 most appropriate according to the measurement area of the
 637 TOP 100 from the SPECTRO 320 spectrometer. Similarly
 638 to the performance in the VIS range, no remarkable differences
 639 were detected between the different ROIs in the IR range.
 640 Consequently, only the results related to the full ROI
 641 are shown.

642 These results also proved the good performance of the de-
 643 veloped system in the IR range, although they were less accurate
 644 than in the VIS range due to the lower density of spectral bands,
 645 the greater spacing among them, and their wider FWHMs.
 646 Focusing on the results, the mean values of the MAEs and
 647 the RMSEs were below 0.07 and especially small in the case
 648 of the solid samples. The mean GFCs were above 0.9500, with

649 the higher values obtained for the metallic samples just below
 650 0.9950; therefore, the highest categories of the GFC scale were
 651 not reached in the IR. Results from the two ROIs revealed
 652 similar outcomes. Additionally, the geometries nearer to
 653 the specular reflection again caused the larger differences
 654 ($45^\circ \times -30^\circ$, $15^\circ \times :0^\circ$). Similarly, the values shown in Fig. 9
 655 were calculated from the three measurement geometries.

656 Although the evaluation of goniochromatic pigments in the
 657 IR range is not common practice, it can provide useful spectral
 658 data on deeper layers of coatings, as well as additional informa-
 659 tion about visual effects that do not produce glint, such as
 660 graininess and mottling. Preliminary data obtained with the
 661 developed system have revealed that sparkling effects are
 662 extremely diminished in this region of the electromagnetic
 663 spectrum, and, therefore, they would not interfere with the as-
 664 sessment of other spatial phenomena such as those previously
 665 mentioned. For instance, IR light could also be used for the
 666 study of graininess instead of or in addition to diffuse VIS light.

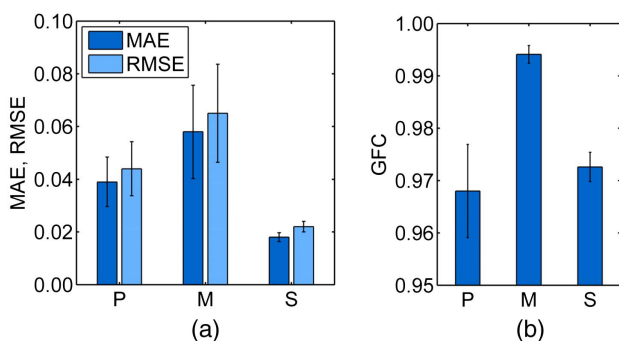
667 5. CONCLUSIONS

668 A gonio-hyperspectral imaging system based on LEDs has been
 669 developed and validated for the analysis of automotive coatings.
 670 The design conforms to the standards DIN 6175-2, ASTM
 671 E2194, and ASTM E2539 for multi-angle color measurement
 672 of goniochromatic pigments.

673 The system provided precise reconstructions of spectral re-
 674 flectances when compared to commercial devices in the IR
 675 (SPECTRO 320) and especially in the VIS range (BYK-mac
 676 and X-Rite). The differences would decrease if both spectral
 677 ranges had similar density of spectral bands, similar spectral
 678 steps, and similar FWHMs. Unfortunately, current solid-state
 679 technology does not provide LEDs above 800 nm with these
 680 features. Similarly, color differences were smaller compared
 681 with the BYK-mac, although deviations with respect to the
 682 X-Rite were lower than for the previous metrics. In general,
 683 the mean CIEDE2000 values were within recommended tol-
 684 erance ranges and smaller than the higher values of the
 685 AUDI2000 due mainly to the solid pigments.

686 A thorough examination of the correlations obtained with
 687 the whole spectral range revealed that the different ROIs
 688 showed analogous results. Another shared outcome was that
 689 the most sensitive geometries were those closer to the specular
 690 reflection, $45^\circ \times -60^\circ$, $45^\circ \times -30^\circ$, $15^\circ \times -30^\circ$, and $15^\circ \times :0^\circ$
 691 for the VIS and $45^\circ \times -30^\circ$ and $15^\circ \times :0^\circ$ for the IR.

692 Lastly, one of the main advantages of the GOHYLED
 693 system is the inclusion of the spectral analysis in the two ranges
 694 of the electromagnetic spectrum, VIS and IR, and for all
 695 the measurement geometries recommended for the characteri-
 696 zation of goniochromatic pigments [6–8]. Currently, the
 697 GOHYLED system is the only instrument with these attrib-
 698 utes. Ongoing research focuses on the assessment of spatial
 699 effects such as sparkle, graininess, and mottling under white
 700 light and narrow-band light sources. The higher spatial resolu-
 701 tion offered by the GOHYLED system in comparison with
 702 other instruments makes it particularly suitable for this task.
 703 Further studies will compare these results with those obtained
 704 by means of psychophysical experiments to accurately validate
 705 the performance of the GOHYLED system.



F9:1 **Fig. 9.** Mean values of (a) MAEs and RMSEs and (b) GFCs for the
 F9:2 spectral reconstruction of the GOHYLED system for the full ROI
 F9:3 with respect to the SPECTRO 320. The three metrics were plotted
 F9:4 for pearlescent (P), metallic (M), and solid (S) samples. The error bars
 F9:5 represent the standard error.

706 **Funding.** Ministerio de Ciencia, Tecnología e Innovación
707 Productiva (MINCyT) (DPI2011-30090-C02); European
708 Union.

709 **Acknowledgment.** Francisco J. Burgos-Fernández
710 thanks the Government of Catalonia for his Ph.D. grant.

711 REFERENCES

- 712 1. P. Bamfield, *Chromic Phenomena* (Royal Society of Chemistry,
713 2001).
- 714 2. F. J. Maile, G. Pfaff, and P. Reynnders, "Effect pigments—past, present
715 and future," *Prog. Org. Coat.* **54**, 150–163 (2005).
- 716 3. G. Pfaff, *Special Effect Pigments: Technical Basics and Applications*,
717 2nd ed. (William Andrew, 2008).
- 718 4. G. Buxbaum and G. Pfaff, *Industrial Inorganic Pigments*, 3rd ed.
719 (Wiley-VCH, 2005).
- 720 5. E. Perales, E. Chorro, V. Viqueira, and F. M. Martínez-Verdú,
721 "Reproducibility comparison among multiangle spectrophotometers,"
722 *Color Res. Appl.* **38**, 160–167 (2012).
- 723 6. DIN 6175-2, "Tolerances for automotive paints—Part 2:
724 Goniochromatic paints" (DIN Deutsches Institut für Normung, 2001).
- 725 7. ASTM Standard E2194-09, "Standard practice for multiangle color
726 measurement of metal flake pigmented" (ASTM International, 2009).
- 727 8. ASTM Standard E2539-08, "Standard practice for multiangle color
728 measurement of interference pigments" (ASTM International, 2008).
- 729 9. A. M. Rabal, A. Ferrero, J. Campos, J. L. Fontecha, A. Pons, A. M.
730 Rubiño, and A. Corróns, "Automatic gonio-spectrophotometer for
731 the absolute measurement of the spectral BRDF at in- out-of-plane
732 and retroreflection geometries," *Metrologia* **49**, 213–223 (2012).
- 733 10. H. Li, S. C. Foo, K. E. Torrance, and S. H. Westin, "Automated three-
734 axis gonioreflectometer for computer graphics applications," *Opt. Eng.*
735 **45**, 043605 (2006).
- 736 11. J. Liu, M. Noël, and J. Zwinkels, "Design and characterization of a
737 versatile reference instrument for rapid, reproducible specular gloss
738 measurements," *Appl. Opt.* **44**, 4631–4638 (2005).
- 739 12. M. E. Nadal and E. A. Thompson, "NIST reference gonio-photometer
740 for specular gloss measurements," *J. Coat. Technol.* **73**, 73–80
741 (2001).
- 742 13. D. Combes, I. Moya, S. Jacquemoud, and H. Sinoquet, "Un nouveau
743 dispositif de mesure des propriétés optiques spectrales et bidirection-
744 nelles de surfaces végétales (Thème n°4)," in *8th International
745 Symposium Physical Measurements & Signatures in Remote
746 Sensing*, Aussois, France, 2001, pp. 283–284.
- 747 14. H. Haneishi, T. Iwanami, N. Tsumura, and Y. Miyake, "Goniospectral
748 imaging of 3D objects," in *Sixth Color Imaging Conference: Color
749 Science, Systems and Applications*, Scottsdale, Arizona, 1998,
750 pp. 173–176.
- 751 15. K. Tonsho, Y. Akao, N. Tsumura, and Y. Miyake, "Development of
752 gonio-photometric imaging system for recording reflectance spectra
753 of 3D objects," *Proc. SPIE* **4663**, 370–378 (2001).
- 754 16. T. Senzaki, Y. Harada, K. Ishikura, J. Hayashi, N. Tsumura, and Y.
755 Miyake, "Development of gonio-spectral imaging software for highly
756 accurate digital archive system," *Jpn. Hardcopy* **2002**, 490–491
757 (2002).
- 758 17. Y. Akao, N. Tsumura, P. G. Herzog, Y. Miyake, and B. Hill,
759 "Gonio-spectral imaging of paper and cloth samples under oblique
760 illumination conditions based on image fusion techniques," *J. Imaging
761 Sci. Technol.* **48**, 227–234 (2004).
- 762 18. A. Kimachi, "Development and calibration of a gonio-spectral imaging
763 system for measuring surface reflection," *IEICE Trans. Inf. Syst.*
764 **E89-D**, 1994–2003 (2006).
- 765 19. E. Perales, E. Chorro, V. Viqueira, and F. M. Martínez-Verdú,
766 "Reproducibility comparison among multiangle spectrophotometers,"
767 *Color Res. Appl.* **38**, 160–167 (2013).
- 768 20. D. B. Kim, M. K. Seo, K. Y. Kim, and K. H. Lee, "Acquisition and
769 representation of pearlescent paints using an image-based gonio-
770 spectrophotometer," *Opt. Eng.* **49**, 043604 (2010).
- 771 21. M. R. Pointer, N. J. Barnes, M. J. Shaw, and P. J. Clarke, "A new
772 goniospectrophotometer for measuring gonio-apparent materials,"
773 *Coloration Technol.* **121**, 96–103 (2005).
- 774 22. H. Andrews and H. Hou, "Cubic splines for image interpolation and
775 digital filtering," *IEEE Trans. Acoust. Speech Signal Process.* **26**,
776 508–517 (1978).
- 777 23. J. Kiusalaas, *Numerical Methods in Engineering with MATLAB*
778 (Cambridge University, 2005).
- 779 24. A. Kurekin, V. Lukin, A. Zelensky, P. Koivisto, J. Astola, and K.
780 Saarinen, "Comparison of component and vector filter performance
781 with application to multichannel and color image processing," in
782 *Proceedings of the IEEE-EURASIP Workshop on Nonlinear Signal
783 and Image Processing (NSIP'99)*, Antalya, Turkey, 1999, pp. 38–42.
- 784 25. J. Farifteh, F. Van der Meer, C. Atzberger, and E. J. M. Carranza,
785 "Quantitative analysis of salt-affected soil reflectance spectra: a com-
786 parison of two adaptive methods (PLSR and ANN)," *Remote Sens.
787 Environ.* **110**, 59–78 (2007).
- 788 26. F. H. Imai, M. R. Rosen, and R. S. Berns, "Comparative study of met-
789 rics for spectral match quality," in *CGIV 2002: The First European
790 Conference on Colour Graphics, Imaging, and Vision*, Poitiers,
791 France, 2002, pp. 492–496.
- 792 27. J. Hernández-Andrés, J. Romero, and R. L. Lee, "Colorimetric
793 and spectroradiometric characteristics of narrow-field-of-view
794 clear skylight in Granada, Spain," *J. Opt. Soc. Am. A* **18**, 412–420
795 (2001).
- 796 28. J. Herrera-Ramirez, M. Vilaseca, F. J. Burgos, L. Font, R. Senserrich,
797 and J. Pujol, "Artwork imaging from 370 to 1630 nm using a novel
798 multispectral system based on light-emitting diodes," *Color Res.
799 Appl.* **40**, 398–407 (2015).
- 800 29. J. Schanda, *Colorimetry: Understanding the CIE System* (Wiley,
801 2007).
- 802 30. N. Ohta and A. R. Robertson, *Colorimetry: Fundamentals and
803 Applications* (Wiley, 2005).
- 804 31. M. R. Luo, G. Cui, and B. Rigg, "The development of the CIE 2000
805 colour-difference formula: CIEDE2000," *Color Res. Appl.* **26**, 340–
806 350 (2001).
- 807 32. Commission Internationale de l'Éclairage, "Improvement to industrial
808 colour-difference evaluation, CIE 142-2001," Tech. rep. (CIE Central
809 Bureau, 2001).
- 810 33. T. Dauser, "Audi color tolerance formulas," Tech. rep. (AUDI AG,
811 2012).
- 812 34. P. Capilla, J. Artigas, and J. Pujol, *Fundamentos de colorimetría*
813 (Universitat de València, 2002).
- 814 35. M. Melgosa, A. Trémeau, and G. Cui, "Colour difference evaluation,"
815 in *Advanced Color Image Processing and Analysis* (Springer, 2013),
816 pp. 65–85.
- 817 36. E. Chorro, E. Perales, F. J. Burgos, O. Gómez, M. Vilaseca, V.
818 Viqueira, J. Pujol, and F. M. Martínez-Verdú, "The minimum number
819 of measurements for colour, sparkle, and graininess characterisation
820 in gonio-apparent panels," *Coloration Technol.* **131**, 303–309
821 (2015).
- 822 37. N. Dekker, E. J. J. Kirchner, R. Supèr, G. J. van den Kieboom, and R.
823 Gottenbos, "Total appearance differences for metallic and pearlescent
824 materials: contributions from color and texture," *Color Res. Appl.* **36**,
825 4–14 (2011).
- 826 38. E. J. J. Kirchner and J. Ravi, "Setting tolerances on color and texture
827 for automotive coatings," *Color Res. Appl.* **39**, 88–98 (2014).